

## ESR and Reflectance Spectra of Manganese in Polycrystalline TiO<sub>2</sub> (Rutile)

D. CORDISCHI,\* M. VALIGI, D. GAZZOLI, AND V. INDOVINA

*Centro di Studio su "Struttura ed Attività Catalitica di Sistemi di Ossidi", Istituto Chimico, Università di Roma, Roma, Italy, and \*Laboratorio Applicazioni in Agricoltura del C.N.E.N. Centro Studi Nucleari della Casaccia, Roma, Italy*

Received December 5, 1974

The ESR and reflectance spectra of polycrystalline TiO<sub>2</sub> containing manganese oxide (up to 8% atomic ratio) have been investigated. The results show that there is only a limited solubility of substitutional Mn<sup>4+</sup> in TiO<sub>2</sub>. The manganese ions are isolated, since the solubility limit prevents clustering of Mn<sup>4+</sup> in TiO<sub>2</sub> matrix. Manganese in excess (with respect to the solubility value) is present as MnTiO<sub>3</sub>. The electronic spectrum of Mn<sup>4+</sup> in the rutile lattice is discussed on the basis of the behavior of isoelectronic Cr<sup>3+</sup> in solid solution in TiO<sub>2</sub>.

### Introduction

Polycrystalline diamagnetic oxides containing transition metal ions have been shown to be useful systems in the investigation of relevant aspects of solid state chemistry and heterogeneous catalysis (1). Among others, systems of interest are those based on titanium dioxide (rutile form) and in our laboratory attention has been focused on TiO<sub>2</sub>-MnO<sub>x</sub>. In a previous paper manganese-doped TiO<sub>2</sub> was characterized by means of X-ray, thermogravimetric, and magnetic techniques and it was found that Mn<sup>4+</sup> enters into the TiO<sub>2</sub> lattice (2). In the present article manganese-containing rutile has been studied by means of electron spin resonance (ESR) and optical methods to detect directly the Mn<sup>4+</sup> in solid solution and to investigate further the interactions and site symmetry of the magnetic ions.

The ESR spectrum of a manganese-doped TiO<sub>2</sub> single crystal has been discussed (3, 4); however, the study has been confined to low manganese content (0.01%) and information on powdered samples is still lacking. Moreover, although several studies on the optical properties of Mn<sup>4+</sup> ions dispersed

in a host lattice such as  $\alpha$ -Al<sub>2</sub>O<sub>3</sub> (5) or Y<sub>3</sub>Al<sub>5</sub>O<sub>8</sub> (6) have been reported, the spectrum of Mn<sup>4+</sup> in TiO<sub>2</sub> has not yet been investigated. Note that the absorption spectrum of the isoelectronic ion Cr<sup>3+</sup> in solid solution in TiO<sub>2</sub> has been studied recently (7, 8). It has been shown that the spectrum cannot be explained in the same way as that for Cr<sup>3+</sup> incorporated into oxides as MgO (9) or  $\alpha$ -Al<sub>2</sub>O<sub>3</sub> (10).

### Experimental Procedure

#### Materials

The samples were prepared by impregnation of titanium oxide (obtained by hydrolyzing TiCl<sub>3</sub>) with manganese nitrate solution. After drying at 393°K the specimens were mixed, ground, calcined in air for 5 hr at 1273°K, and finally quenched in air to room temperature. The specimens are designated as *TM*, the figure after the letters giving the nominal concentration of manganese atoms with respect to 100 Ti atoms. Pure TiO<sub>2</sub> was prepared by the same heat treatment excluding the impregnation step. Details of sample characterization are reported elsewhere (2); Table I summarizes the samples studied. The

TABLE I  
ANALYTICAL DATA AND CRYSTALLINE PHASES FOR  
TiO<sub>2</sub> CONTAINING MANGANESE OXIDE

Samples <sup>a</sup>	Mn <sub>tot</sub> <sup>b</sup>	Mn <sup>4+</sup> <sup>b</sup>	Crystalline phase
TM 0.1	—	—	Rutile
TM 0.5	0.51	0.45	Rutile
TM 0.7	0.70	0.66	Rutile
TM 2	1.89	0.95	Rutile + MnTiO <sub>3</sub>
TM 4	4.52	1.24	Rutile + MnTiO <sub>3</sub>
TM 7	6.72	1.24	Rutile + MnTiO <sub>3</sub>
TM 8	8.30	1.24	Rutile + MnTiO <sub>3</sub>

<sup>a</sup> For key to designation of samples see text.

<sup>b</sup> Manganese atoms/100 titanium atoms.

X-ray patterns of samples *TM* 0.1, *TM* 0.5, and *TM* 0.7 gave no evidence for the presence of phases different than TiO<sub>2</sub>. The X-ray spectra of sample *TM* 2 and those of more concentrated specimens showed the lines of MnTiO<sub>3</sub> in addition to the rutile reflections. Samples containing chromium and iron were prepared by the same procedure. These samples are indicated as *TC* 0.1 and *TF* 0.1, respectively.

#### ESR and Optical Measurements

ESR were recorded at room and liquid nitrogen temperatures on Varian E-9 spectrometer, operating at X-band frequencies, with 100 kHz of field modulation. Relative intensities were determined by comparing the area obtained by double integration of the first derivative spectrum for the samples with that for a standard of a CuSO<sub>4</sub>·5H<sub>2</sub>O single crystal.

Diffuse reflectance spectra in the range 2500–350 nm were obtained with a Beckman DK-1 spectrophotometer, at room temperature. Some spectra were also recorded at liquid nitrogen temperature. The specimens were analyzed using MgO as reference.

## Results

### ESR

Figure 1 shows the spectrum of sample *TM* 0.1. This spectrum consists of a double

sixtet of lines centered at  $H_1 \simeq 1220$  G ( $\nu_0 = 9.53$  GHz). The sextets have slightly different total splittings (392 G and 380 G, respectively). In the region  $g \simeq 2$ , two other sextets centered at  $H_2 = 3270$  G and  $H_3 = 3470$  G, respectively, are present. The total splittings of these two sextets are practically equal to 390 G. A further sextet of very low intensity, centered at  $H_4 \simeq 8300$  G (not shown in Fig. 1a), is observable.

The spectrum is slightly modified when recorded at liquid nitrogen temperature. Besides better resolution, a shift of the sextet centered at  $H_2$  is observed. This shift amounts to 150 G in the direction of lower fields. Therefore, the separation between the two sextets in the region  $g \simeq 2$  becomes 350 G. The hyperfine splittings remain unchanged.

Figures 1b and 1c show the spectra of Cr<sup>3+</sup> (*TC* 0.1) and Fe<sup>3+</sup> (*TF* 0.1) in the same matrix. Fig. 1d refers to the spectrum of undoped TiO<sub>2</sub>. Comparing the spectra shown in Fig. 1, it is deduced that the titanium dioxide used in the preparation of the *TM* samples contains Fe<sup>3+</sup> as the predominant paramagnetic impurity. The amount of Fe<sup>3+</sup> has been estimated to be ~100 ppm, i.e., one order of magnitude lower than the manganese content in *TM* 0.1.

The assignment of the resonance lines, as indicated under each spectrum, has been performed employing the parameters of the spin Hamiltonian obtained from single crystal studies on these systems (3, 4, 11, 12) and using the diagram reported by Van Reijen (13) for  $d^3$  ions and by Aasa (14) for  $d^5$  ions. As an example,  $Y_{12}$  indicates the resonance line ascribed to the transition  $1 \leftrightarrow 2$ , the  $Y$ -axis of the crystal being parallel to the magnetic field. In this way all details of the ESR spectra can be interpreted. The analysis has been carried out not only for Mn<sup>4+</sup> in rutile, the powder spectrum of which has not yet been reported in the literature, but also for Cr<sup>3+</sup> and Fe<sup>3+</sup> in the same matrix. In any case, there is close agreement between the theoretical and experimental positions of each resonance line, providing an unambiguous identification of the paramagnetic species.

Figure 2 shows the influence of the man-

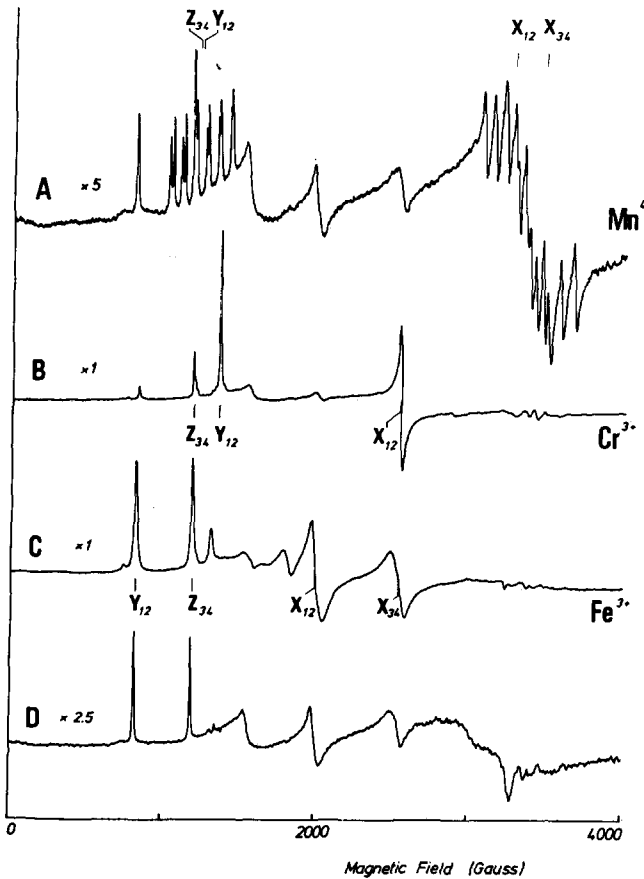


FIG. 1. ESR spectra at X-band of powdered  $\text{TiO}_2$  samples at room temperature: A = *TM* 0.1; B = *TC* 0.1;  $C_{\text{Mn}} = \text{TF}$  0.1; D = undoped  $\text{TiO}_2$ . For each spectrum the numbers indicate the relative gains. For symbols of resonance lines see text.

ganes concentration on the ESR spectrum. The increase of total manganese content causes strong changes in the spectrum. The sextet centered at 1220 G is present in all the samples, but is resolved into a double sextet only at the lowest concentration. Its intensity increases with the manganese content up to sample *TM* 0.75, and then remains practically constant (Fig. 3). In addition, the sextets in the region  $g \simeq 2$  become less resolved with increase in manganese content. For the *TM* 0.75 sample, the hyperfine structure is still observable, while for specimens with higher manganese content the hyperfine structure is absent (Fig. 2). In these more concentrated samples there is an intense

symmetric line that is structureless and Lorentzian in shape. The width of this line decreases as the manganese concentration increases. At liquid nitrogen temperature this line broadens. Fig. 4 shows the signal intensity, integrated over a range of 4000 G versus the manganese content. The integrated intensity is linearly dependent on the manganese content. The straight line intercepts the concentration axis at  $\sim 1$  manganese atoms per 100 Ti atoms.

#### Optical Spectra

Figure 5 shows the absorption spectra of some samples (the base line has been shifted

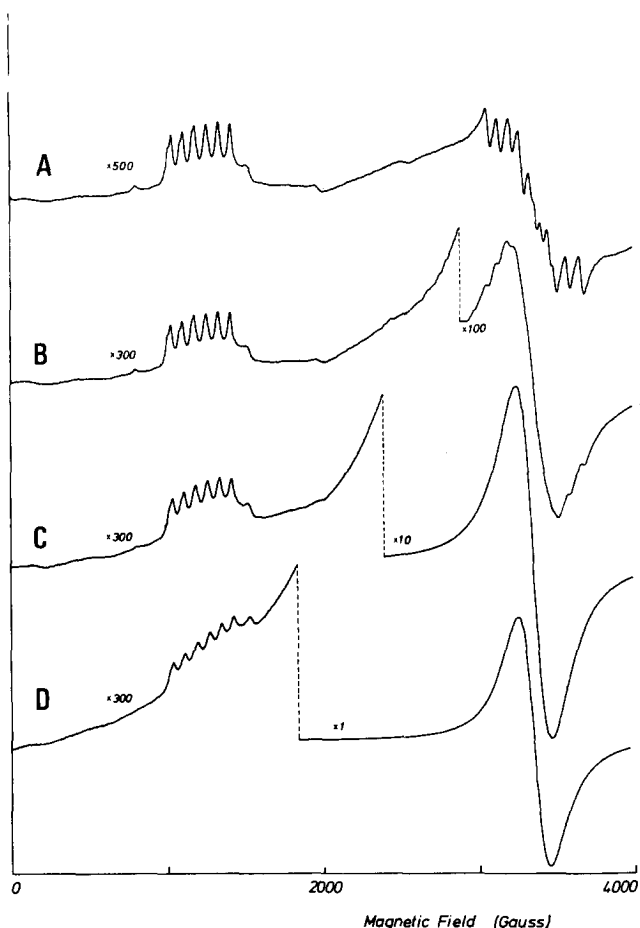


FIG. 2. ESR spectra at X-band of *TM* samples at room temperature: A = *TM* 0.5; B = *TM* 0.75; C = *TM* 2; D = *TM* 8. For each portion of the spectra the numbers indicate the relative gains. For symbols of resonance lines see text.

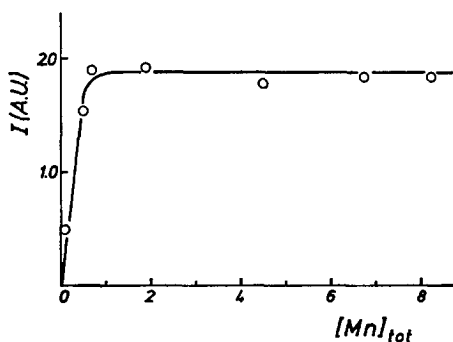


FIG. 3. Intensity (arbitrary units) of the sextet at  $H_1 \approx 1220$  G for the *TM* samples versus total manganese content,  $[\text{Mn}]_{\text{tot}}$ .  $[\text{Mn}]_{\text{tot}} = \text{Mn atoms}/100 \text{ Ti atoms}$ .

for clarity). For the undoped  $\text{TiO}_2$ , a band at  $26\,000 \text{ cm}^{-1}$  is observed. This band corresponds to the fundamental absorption of rutile (15). The addition of manganese modifies the  $\text{TiO}_2$  absorption. In fact, two bands occur: the first, weak, is centered at  $16\,000 \text{ cm}^{-1}$ ; the second, broad and intense at  $22\,000 \text{ cm}^{-1}$  is not resolved from the fundamental absorption of  $\text{TiO}_2$ . Both bands increase in intensity as the manganese concentration increases. The spectra recorded at liquid nitrogen temperature did not differ appreciably from those obtained at room temperature.

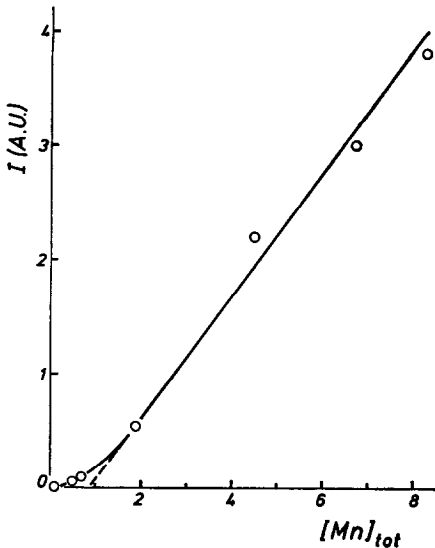


FIG. 4. Integrated intensity (arbitrary units) of the signal at  $g \simeq 2$  versus the total manganese content,  $[Mn]_{tot}$ .  $[Mn]_{tot} = \text{Mn atoms}/100 \text{ Ti atoms}$ .

## Discussion

### ESR

The analysis of the ESR spectra confirms the fact that the manganese is slightly soluble in the  $\text{TiO}_2$  lattice and is incorporated substitutionally as magnetically isolated  $\text{Mn}^{4+}$  ions. This result, previously deduced from thermogravimetric and lattice parameter measurements, and from determinations of the magnetic susceptibility (2), now receives direct spectroscopic confirmation. The assignment of the bands in more dilute samples clearly shows that the ESR spectrum with hyperfine structure is due to isolated  $\text{Mn}^{4+}$  ions at  $\text{Ti}^{4+}$  sites. Indeed, all information obtained from the single-crystal study is also deducible from the powder spectra of the more diluted samples. As an example, the small anisotropy of the hyperfine tensor is easily measurable and the slight variation of the parameter  $\varepsilon = |E||D|$  with temperature [from 0.320

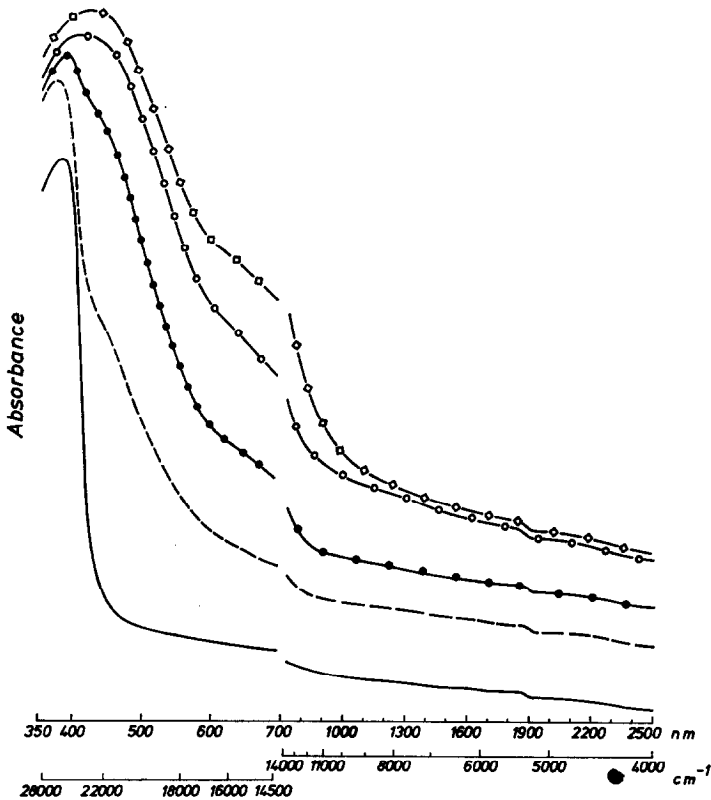


FIG. 5. Diffuse reflectance spectra of TM samples: — undoped  $\text{TiO}_2$ ; - - -  $TM\ 0.1$ ; —●—●—  $TM\ 0.2$ ; —○—○—  $TM\ 0.5$ ; —◇—◇—  $TM\ 4$ .

at room temperature to 0.308 at 77°K, as observed by Andresen on a TiO<sub>2</sub> single crystal (3, 4)], is responsible for the modification with temperature of the spectrum in the region  $g \simeq 2$ . As the manganese content increases, the limit of solubility of Mn<sup>4+</sup> in TiO<sub>2</sub> is reached and a new phase forms. Hence, while the hyperfine sextet centered at  $H_2 \simeq 1220$  G persists, the structure in the region  $g \simeq 2$  disappears (Fig. 2).

Note that from the analysis of some features of the single line that develops in this region (shape, line width, dependence on the temperature, intensity variation with the manganese content) it may be deduced that manganese species different from isolated Mn<sup>4+</sup> ions are formed. However, since the signal observed in the region  $g \simeq 2$  could be due to different paramagnetic species, such as Mn<sup>4+</sup> and Mn<sup>2+</sup>, the only possible deduction is that at increasing manganese content the Mn<sup>2+</sup> and/or Mn<sup>4+</sup> ions become associated. On the other hand, the X-ray analysis shows that for samples at higher manganese content (Table I) the MnTiO<sub>3</sub> segregates so that the single symmetric line present in more concentrated samples is assigned to the Mn<sup>2+</sup> in this phase. Obviously, when the intensity of this line is very much larger than that due to the isolated Mn<sup>4+</sup> ions, the hyperfine structure in the region  $g \simeq 2$  is no longer detectable. Nevertheless, the presence of these ions is demonstrated by the sextet centered at  $H_1 \simeq 1220$  G (Fig. 2).

When paramagnetic ions are dispersed in a diamagnetic matrix to form a homogeneous solid solution the concentration of the isolated ions increases, reaches a maximum, and then decreases. The intensity of the ESR signal due to these ions parallels this behavior. After the maximum is reached, the intensity decreases and finally disappears completely (16, 17). For high concentration, a different ESR signal, caused by clustering of paramagnetic ions, is usually observed. This signal is characterized by the absence of fine and hyperfine structure and is generally narrowed by exchange effects. The value of the concentration corresponding to the intensity maximum of the signal of the isolated ions depends on the nature of the matrix and the para-

magnetic ion, on their distribution, and on the type of site occupied. It has been shown (16, 17) that for a random distribution of the paramagnetic ion the maximum is located at about 1% atomic ratio. Contrary to this expected behavior, the intensity of the ESR signal of the isolated Mn<sup>4+</sup> ions does not decrease after this value, but remains constant (Fig. 3). In our system, the solubility limit is close to 1% [1.24 atomic ratio (2)] so that the increase of total manganese concentration does not entail clustering of the Mn<sup>4+</sup> ions in the TiO<sub>2</sub> matrix.

As shown in Table I, in more concentrated samples the major part of the manganese is present as Mn<sup>2+</sup> in the titanate phase. This is also inferred from Fig. 4. As the manganese content increases, the contribution in the ESR spectrum of Mn<sup>4+</sup> with respect to Mn<sup>2+</sup> becomes negligible for several reasons: (1) The fraction of Mn<sup>4+</sup> with respect to the Mn<sup>2+</sup> decreases; (2) the spin of Mn<sup>4+</sup> is  $\frac{3}{2}$ , whereas that of Mn<sup>2+</sup> is  $\frac{5}{2}$ ; and (3) the anisotropy of Mn<sup>4+</sup> broadens the spectrum in a wide region of magnetic field. In Fig. 4, the straight line intercepts the manganese content axis at  $\sim 1\%$  atomic value, which agrees with the solubility limit determined previously (2).

An estimate of the absolute concentration of Mn<sup>2+</sup> present in more concentrated samples, deduced from the intensity of the integrated spectra with respect to CuSO<sub>4</sub>·5H<sub>2</sub>O as standard, agrees with the analytical values within a factor of two. Due to the larger possibility of error in this kind of measurement the agreement is satisfactory. Thus, almost all of the Mn<sup>2+</sup> ions in the titanate phase contribute to the ESR spectrum in the region  $g \simeq 2$ .

### Optical Spectra

The previous arguments clearly show that Mn<sup>4+</sup> is present in a TiO<sub>2</sub> matrix. Thus, it seems reasonable to attempt a correlation between the Mn<sup>4+</sup> in the TiO<sub>2</sub> structure and the optical absorption of TM samples (Fig. 5). However, several points must be emphasized first. Wittke (18) observed that when transition metal ions are introduced into rutile the absorption edge of the titanium oxide is

shifted toward the red. The same phenomenon was observed by Johnson, Ohlsen, and Kingsbury (19) when  $\text{TiO}_2$  contains iron and donor impurity. It may be recalled that a broad intense band in the visible region, similar to that observed in the spectra of our *TM* samples has been reported for a rutile single crystal containing  $\text{Cr}^{3+}$  (7). In the same study, it was reported that a similar absorption also occurs when  $\text{SrTiO}_3$  and  $\text{CaTiO}_3$  are doped with  $\text{Cr}^{3+}$ ,  $\text{Fe}^{3+}$ , and  $\text{Co}^{3+}$  and the authors concluded that the band arises from defects induced by the dopant. This conclusion agrees with the observation that the intensity of the band is related to the  $\text{Cr}^{3+}$  concentration. We propose that the band recorded in the region  $22\,000\text{ cm}^{-1}$  is similar in nature to that observed in  $\text{Cr}^{3+}$  in  $\text{TiO}_2$  (7), being due to some defects induced by the addition of manganese.

By contrast, the absorption at  $16\,000\text{ cm}^{-1}$  is believed a *d-d* transition. Following Grabner, Stokowski, and Brower (7), the spectrum of  $\text{Cr}^{3+}$  in  $\text{TiO}_2$  shows a band centered at  $13\,800\text{ cm}^{-1}$ . The absorption is ascribed to the  ${}^4A_2 \rightarrow {}^4T_1$  transition. The proposed assignment is rather unusual. In fact, this transition in the case of  $\text{Cr}^{3+}$  in oxides such as  $\text{MgO}$  (9) or  $\alpha\text{-Al}_2\text{O}_3$  (10) is located at  $16\,000\text{ cm}^{-1}$  and  $18\,000\text{ cm}^{-1}$ , respectively. However, this type of assignment as been confirmed recently via an investigation on the Zeeman effect (8).

Recalling that  $\text{Mn}^{4+}$  is isoelectronic with  $\text{Cr}^{3+}$ , it is plausible to suggest that the two ions dissolved in the same matrix show similar optical behavior. Since the  $\text{Mn}^{4+}$  ion has an effective positive charge greater than  $\text{Cr}^{3+}$ , the absorption band occurs at higher energy ( $16\,000\text{ cm}^{-1}$ ).

## Acknowledgments

The authors wish to thank Prof. A. Cimino for useful discussion and critical reading of the manuscript.

## References

1. A. CIMINO, *Chim. Ind. (Milan)* **56**, 27 (1974).
2. M. VALIGI AND A. CIMINO, *J. Solid State Chem.*, **12**, 135 (1975).
3. H. G. ANDRESEN, *Phys. Rev.* **120**, 1606 (1960).
4. H. G. ANDRESEN, *J. Chem. Phys.* **35**, 1090 (1961).
5. S. GESCHWIND, P. KISLIUK, M. P. KLEIN, J. P. REMEIKA, AND D. L. WOOD, *Phys. Rev.* **126**, 1684 (1962).
6. L. A. RISEBERG AND M. J. WEBER, *Solid State Chem.* **9**, 791 (1971).
7. L. GRABNER, S. E. STOKOWSKI, AND W. S. BROWER, *Phys. Rev. B* **2**, 590 (1970).
8. L. GRABNER AND E. Y. WONG, *Phys. Rev. B* **8**, 1032 (1973).
9. D. S. MCCLURE, *Solid State Phys.* **9**, 493 (1959).
10. D. S. MCCLURE, *J. Chem. Phys.* **36**, 2757 (1962).
11. H. J. GERRITSEN, S. E. HARRISON, H. R. LEWIS, AND J. P. WITTKKE, *Phys. Rev. Letters* **2**, 153 (1959).
12. A. OKAYA AND D. CARTER, *Phys. Rev.* **118**, 1485 (1960).
13. L. L. VAN REIJEN, Thesis, Amsterdam (1964).
14. R. AASA, *J. Chem. Phys.* **52**, 3919 (1970).
15. A. L. COMPANION AND R. F. WYATT, *J. Phys. Chem. Solids* **24**, 1025 (1963).
16. F. GESMUNDO AND C. DE ASMUNDIS, *J. Phys. Chem. Solids* **34**, 637 (1973).
17. F. GESMUNDO AND C. DE ASMUNDIS, *J. Phys. Chem. Solids* **34**, 1757 (1973).
18. J. P. WITTKKE, *J. Electrochem. Soc.* **113**, 193 (1966).
19. O. W. JOHNSON, W. D. OHLSEN, AND P. I. KINGSBURY, *Phys. Rev.* **175**, 1102 (1968).